Supporting Information

Microporous metal-organic framework with open metal sites and π-Lewis acidic pore surfaces for recovering ethylene from polyethylene off-gas

Yingxiang Ye,[a] Zhenlin Ma,[a] Liangji Chen,[a] Haizhen Lin,[a] Quanjie Lin,[a] Lizhen Liu,[a] Ziyin Li,[a] Shimin Chen,[a] Zhangjing Zhang,*[ab] and Shengchang Xiang*[ab]

[a]*Fujian Provincial Key Laboratory of Polymer Materials, College of Chemistry and Materials Science, Fujian Normal University, 32 Shangsan Road, Fuzhou 350007, PR China*

[b]*State Key Laboratory of Structural Chemistry, Fujian Institute of Research on the Structure of Matter, Chinese Academy of Sciences, Fuzhou, 350002, People's Republic of China*

Corresponding authors E-mail: zzhang@fjnu.edu.cn. E-mail: scxiang@fjnu.edu.cn.

Contents

Table S1. Crystallographic Data and Structural Refinement Summary.

Compounds	**FJU-101**	**FJU-102**
CCDC	1847821	1849673
Empirical formula	$C_{15}H_7CuNO_7$	$C_{19}H_{14}CuN_2O_7$
Formula weight	376.76	445.86
Temperature (K)	150	150
Crystal system	tetragonal	orthorhombic
Space group	*P42$_1$2*	*Imma*
a (Å)	18.2466(3)	15.2262(5)
b (Å)	18.2466(3)	36.4417(13)
c (Å)	16.9110(4)	10.3313(5)
α (°)	90	90
β (°)	90	90
γ (°)	90	90
Volume (Å^3)	5630.3(2)	5732.5(4)
Z	8	8
D_c (g cm^{-3})	0.889	1.033
μ (mm^{-1})	1.296	1.348
F(000)	1512.0	1816.0
Crystal size (mm^3)	0.1×0.1×0.04	0.12×0.1×0.05
Radiation	Cu *Kα* (λ =1.54178Å)	Cu *Kα* (λ =1.54178Å)
Goodness-of-fit on F^2	0.941	1.079
Final *R* indexes [*I*>=2σ (*I*)][(a)]	R_1 = 0.0513, wR_2 = 0.1228	R_1 = 0.0412, wR_2 = 0.1189
Final R indexes [all data] [(a)]	R_1 = 0.0754, wR_2 = 0.1333	R_1 = 0.0479, wR_2 =0.1241

(*a*) $R_1 = \Sigma||F_O| - |F_C|| / \Sigma|F_O|; wR_2 = [\Sigma w(|F_O|^2 - |F_C|^2)^2 / \Sigma w(F_O{}^2)^2]^{1/2}$

Table S2. CO_2 adsorption performances on some representative porous materials under 1 bar.

Materials	S_{BET} (m^2/g)	V_p (cm^3/g)	CO_2 uptake at 273 K (or 298 K) and 1.0 bar		Functional sites	$Q_{st,n=0}$ (kJ mol^{-1})	ref
			cm^3/g	cm^3/cm^3			
ZJU-12a	2316	0.938	243 (134)	194 (107)	OMS	26.9	1
CPM-231	1140	0.564	232.3 (151.6)	213.9 (139.6)	PSP	20.4	2
MgMOF-74	1495	0.572	229 (179.5)[a]	208.4 (162)[a]	OMS	47	3
Cu-TDPAT	1938	0.93	227 (132)	177.8 (103.4)	OMS+LBS	42	4
FJU-101a	1935	0.77	219.1 (130.2)[a]	182.9 (109)[a]	OMS	28.4	This work
Cu-TPBTM	3160	1.27	216.8 (118.5)	135.9 (74.3)	OMS+LBS	26.3	5
JLU-Liu21	2080	1.00	210 (118)	NA	OMS+LBS	28	6
HP-e	1210	0.45	209 (157)	NA	Open O	35.2	7
NJU-Bai21	1979	0.788	206.5 (115.1)	121.2 (72.2)	OMS+LBS	25.9	8
[Cu(Me-4py-trz-ia)]	1473	0.586	206.1 (136.6)[a]	190.2 (5.7)[a]	OMS+LBS	30	9
NOTT-125	2447	1.1	203.6 (92.5)	140.6 (63.9)	OMS+LBS	25.4	10
NbO-Pd-1	1568	0.60	201.8 (124.8)	187.8 (116.2)	OMS	23.5	11
LCu'	1952	0.98	198.5 (98.12)	147.3 (72.8)	OMS+LBS	27.1	12
SNU-5	2850	1.00	196	161.7	OMS+LBS	NA	13
FJI-H14	904	0.45	193.8 (146)	227 (171)	OMS+LBS	26.6	14
SNNU-61	905.2	0.49	161.8 (93.0)	188.2 (108.2)	OMS+LBS	27.0	15
PCN-88	3308	1.599	160 (94)[a]	105.8 (62)[a]	OMS	27	16
MAF-X25ox	1286	0.46	(159)	(195)	OMS+LBS	99	17
CoMOF-74	1080	0.515	(155.8)[a]	(184)[a]	OMS	37	3
MAF-X27ox	1167	0.41	(150)	(203)	OMS+LBS	110	17
SIFSIX-2-Cu-i	735	0.324	145.6 (121.2)	179.2 (151)	LBS	31.9	18
Mg_2(dobpdc)	3270	1.384	(143.8)	(102)	OMS	44	19
HKUST-1	1734	0.848	138.4 (93.8)	121 (82.9)	OMS	35	20
Bio-MOF-11	1040	0.45	134.4 (91.8)	165.8 (113)	OMS+LBS	45	21
NiMOF-74	1070	0.47	(130.3)[a]	(157.1)[a]	OMS	41	3
UTSA-16	628	0.31	(96.9)[a]	(160)[a]	H_2O	34.6	22

[a]296 K.

NA = not available; PSP = pore space partition; OMS = open metal site; LBS = Lewis basic site

Table S3. Ethylene adsorption performances on some representative porous materials.

Materials	Formula[a]	S_{BET} (m^2/g)	V_p[a] (cm^3/g)	d_G[b] (mmol/g)	C_2H_4 uptake at 1.0 bar		T(K)	Q_{st} (kJ/mol)	Ref
					(mmol/g)	(perM)			
FJU-101a	Cu_2(L)	1935	0.77	2.79	6.35	2.28	296	36.1	This work
$Cu_6(DDC)_3$	Cu_2(DDC)	2410	0.98	3.37	7.14	2.12	298	34.7	23
NOTT-102	Cu_2(qptc)	2932	1.2807	2.82	5.8	2.06	296	41	24
Cu-TDPAT	Cu_3(TDPAT)	1938	0.93	3.74	7.34	1.96	298	49.5	25
ZJU-11a	Cu_2(L2)	2531	1.0087	3.69	7.01	1.9	298	36.1	26
ZJU-25a	Cu_2(FDDI)	2124	1.183	3.24	6.05	1.87	296	19.4	27
PCN-16	Cu_2(ebdc)	2273	1.06	4.20	7.14	1.7	296	39.4	24
Cu-TDPAH	Cu_3(TDPAH)	2171	0.91	3.36	5.21	1.55	298	45.0	28
HKUST-1	$Cu_3(BTC)_2$	1781	0.70	4.97	7.4	1.49	296	39.2	24
MOF-505	Cu_2(bptc)	1547	0.60	4.43	5.1	1.15	296	48	24
CoMOF-74	Co_2(dobdc)	1018	0.515	6.42	7.0	1.09	296	40.9	24
FeMOF-74	Fe_2(dobdc)	1350	0.626	6.54	6.02	0.92	318	45	29
MgMOF-74	Mg_2(dobdc)	927	0.607	8.27	7.4	0.895	296	42.2	24
NiMOF-74	Ni_2(dobdc)	1027	0.47	6.39	5.3	0.83	298	NA	30
CuMOF-74	Cu_2(dobdc)	1030	0.43	6.23	4.97	0.798	298	30	30

[a]Guest molecules not included in the formula. [b]d_G are theoretical gravimetric densities of guest-binding metal sites. NA = not available

TDPAT = 2,4,6- tris(3,5-dicarboxylphenylamino)-1,3,5-triazine,

TDPAH = 2,5,8-tris(3,5-dicarboxylphenylamino)-s-heptazine,

H_4DDC = 5,5′-(2,3-dihydrothieno[3,4-b][1,4]dioxine-5,7-diyl)-diisophthalic acid)

H_4L2 = 5,5′-(1-Methylbenzene-2,5-diyl)diisophthalic acid

H_4dobdc = 2,5-dihydroxyterephthalic acid

H_4ebdc = 5,5′-(1,2-ethynediyl)bis(1,3-benzenedicarboxylic acid)

H_4tptc = Terphenyl-3,3″,5,5″-tetracarboxylic acid

H_4qptc = Quaterphenyl-3,3‴,5,5‴-tetracarboxylic acid

H4bptc = Biphenyl-3,3′,5,5′-tetracarboxylic acid

H_4FDDI = tetramethyl 5,5′-(9*H*-fluorene-2,7-diyl)diisophthalate acid

Table S4. Comparison of acetylene adsorption data at ambient condition for some typical MOFs.

Materials	S_{BET} (m^2/g)	V_p[a] (cm^3/g)	ρ (g/cm^3)	C_2H_2 uptake at 1.0 bar		T (K)	$Q_{st,n=0}$ (kJ/mol)	Ref
				(cm^3/g)	(cm^3/cm^3)			
ZJU-12a	2316	0.938	0.799	244	195	298	29	1
FJI-H8	2025	0.82	0.875	224	196	295	32.0	31
NJU-Bai17	2423	0.914	0.787	222.4	175	296	38	32
ZJU-40a	2858	1.06	0.750	216	162	298	34.5	33
ZJNU-47	2638	1.031	0.689	213	146.8	295	35.0	34
ZJNU-54	2134	0.871	0.813	211	171.5	295	35.4	35
Cu_2TPTC-OMe	2278	1.057	0.801	204	163.4	298	19.1	36
HKUST-1	1781	0.70	0.881	201	177	295	34.0	37
NOTT-103	3001	1.157	0.643	199	128	296	30.8	24
ZJU-8a	2501	1.0224	0.687	195	134	298	29.6	38
CoMOF-74	1018	0.515	1.169	197	230.3	295	50.1	39
ZJNU-34(NH_2)	2459	0.9687	0.706	193.8	136.9	298	34.2	40
ZJU-5a	2823	1.074	0.679	193	131	298	35.8	41
SIFSIX-1-Cu	1178	0.57	0.864	190.4	164.5	298	30	42
MgMOF-74	927	0.607	0.909	184	167.2	296	34.0	39
NOTT-101	2755	1.0579	0.657	184	120.8	298	32.8	24
ZJU-7a	2198	0.8945	0.750	180	135	298	28.8	43
Cu-TDPAT	1938	0.93	0.782	178	139.2	298	30.8	25
PCN-16	2273	1.06	0.724	176	127.4	296	34.5	24
FJU-101a	1935	0.77	0.835	172.5	144	296	35.9	This work
ZJU-72a	1184	0.635	0.773	167.7	129.6	298	9.7	44
ZJU-11a	2531	1.0087	0.700	165	115.5	298	36.8	26
$Cu_6(DDC)_3$	2410	0.98	0.757	164	124.1	298	33.5	23
CPM-200-Fe/Mg	1459	0.72	NA	160.8	NA	298	NA	45
Cu-EBTC	1852	1.000	0.772	160	123.5	295	34.5	46
FeMOF-74	1350	0.626	1.126	152	171.2	318	47	29
MOF-505	1547	0.60	0.926	148	137	296	24.7	37
NOTT-102	2932	1.2807	0.587	146	85.7	296	22.0	24
NOTT-300	1370	0.433	1.062	142	150.8	293	32	47
UTSA-100a	970	0.399	1.146	95.6	109.6	296	22	48
SNNU-61	905.2	0.49	1.162	122.2	142.1	298	38.2	15

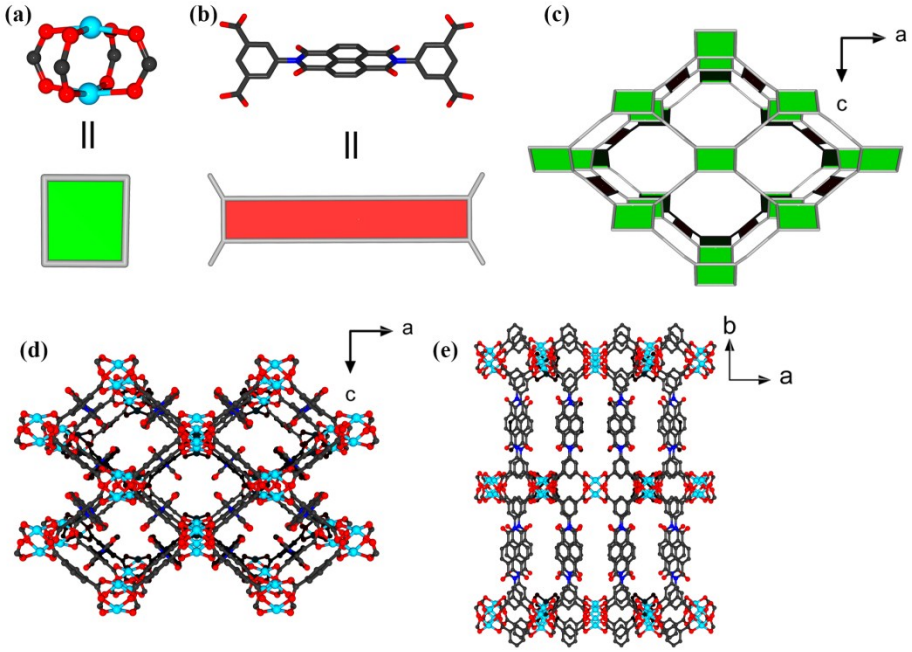

Fig. S1 Description of the structures of **FJU-102**: Illustration of the paddle-wheel unit (a) and the organic ligand H_4L (b), and both of them viewed as planar 4-connected node. (c) Polyhedral view of the ***lvt*** topology network. The 3D framework structure viewed along the (d) *b* axis and (e) *c* axis, respectively. Color scheme: Cu = sky blue, C = dark gray, O = red, N = blue. Guest molecules and H atoms have been omitted for clarity.

Single-crystal X-ray diffraction analysis revealed that **FJU-102** crystallizes in the orthorhombic space group *Imma*. As frequently observed in MOFs, the framework nodes in **FJU-102** consist of paddle-wheel dinuclear $Cu_2(COO)_4$ secondary building units (SBUs) with the organic linkers (H_4L) to form a three-dimensional (3D) framework. From the topological point of view, if the paddle-wheel SBU and organic ligand view as 4-connected square-planar and rectangular-planar, respectively. **FJU-102** adopts the rare ***lvt***-type network with the point (Schläfli) symbol of $\{4^2 \cdot 8^4\}$, which was different from **FJU-101** and well-known ***nbo*** MOFs.[49] The solvent accessible volume in the dehydrated structure is 65.4% calculated from PLATON/SOLV,[50,51] which is slightly larger than that of **FJU-101**.

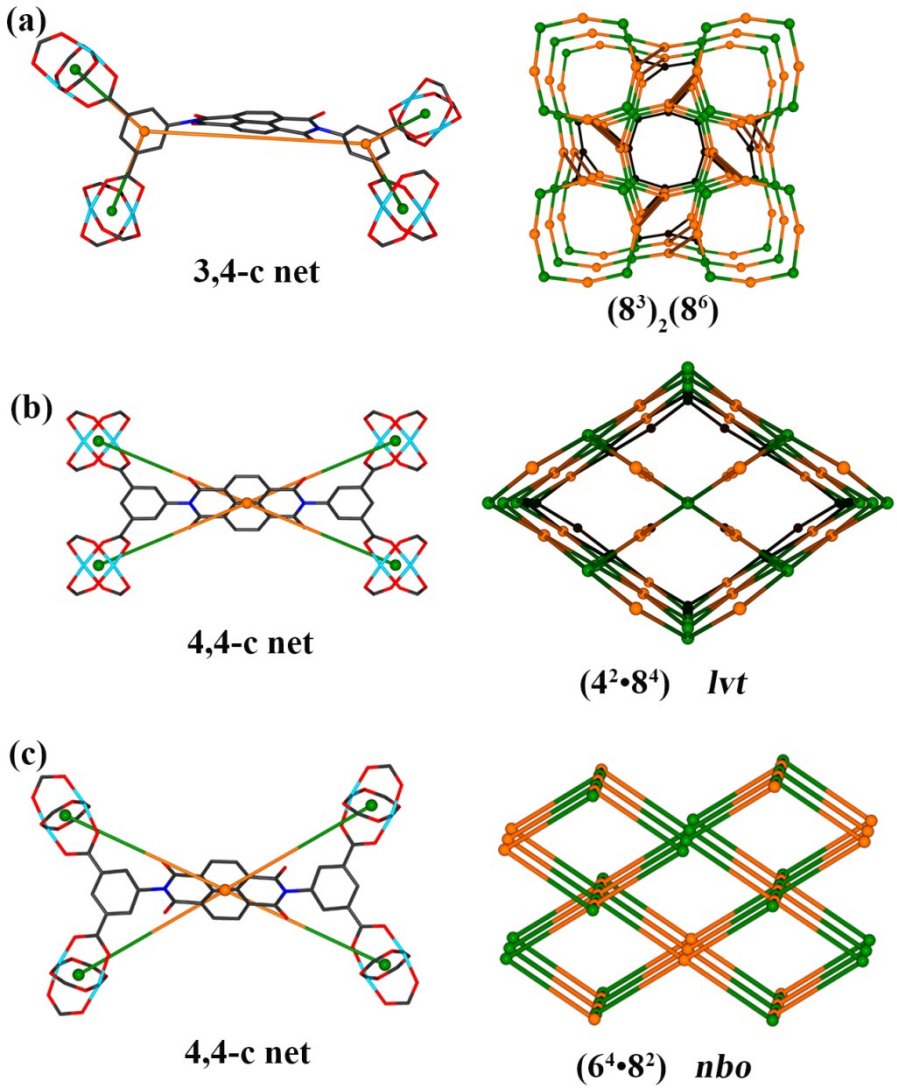

Fig. S2 View of the connected mode between H_4L and $Cu_2(COO)_4$ unit in (a) **FJU-101**, (b) **FJU-102** (***lvt***), and (c) previous reported MOF (***nbo***).[49]

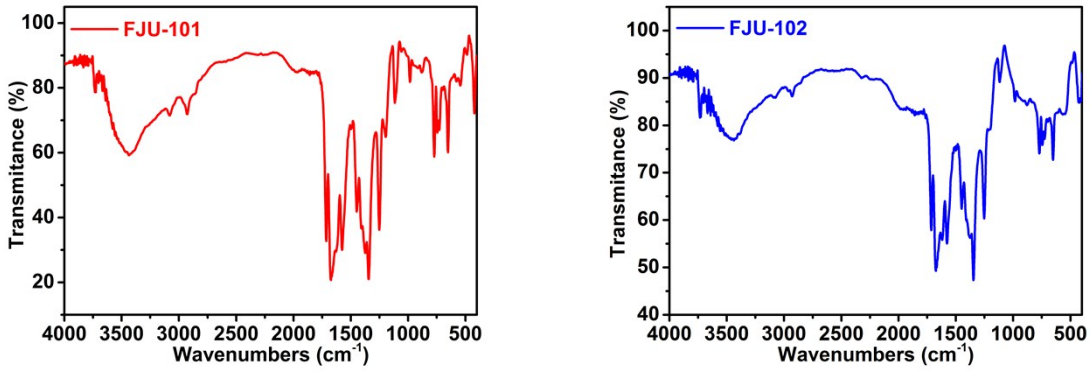

Fig. S3 FT-IR spectra of the as-synthesized samples.

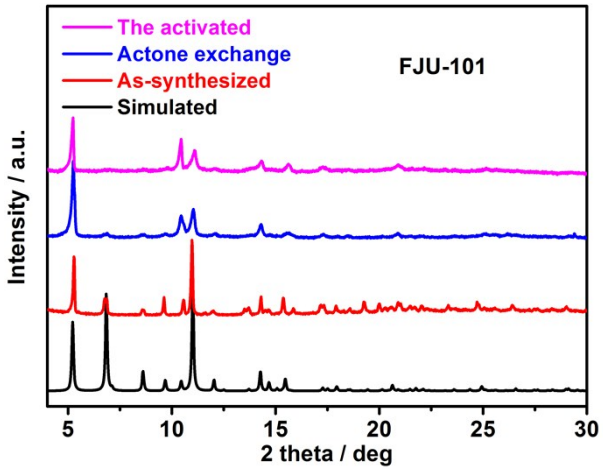

Fig. S4 The powder X-ray diffraction patterns for **FJU-101**.

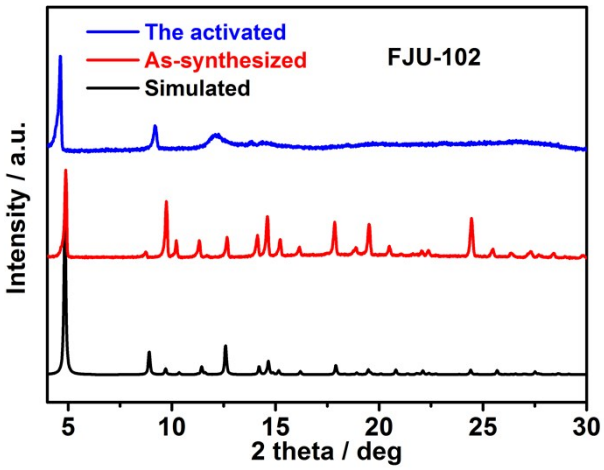

Fig. S5 The powder X-ray diffraction patterns for **FJU-102**.

As shown in Fig. S4 and S5, the experimental PXRD pattern of **FJU-101** and **FJU-102** matches well with that simulated one from the single-crystal data, indicating its pure phase. The difference of powder diffraction peak relative intensity between the simulation and experiment is mainly due to the preferred orientation of the crystallite samples.[52]

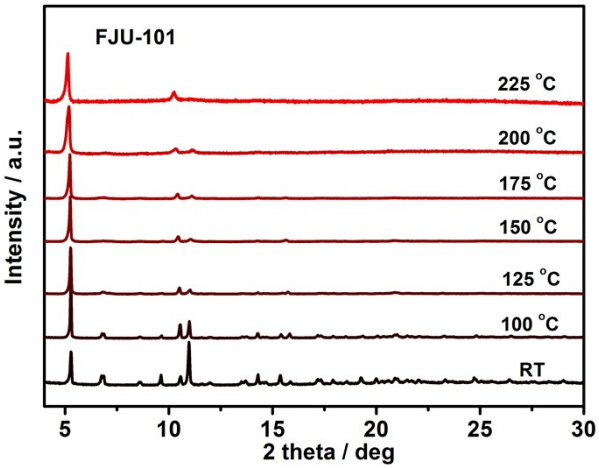

Fig. S6 Variable-temperature powder X-ray diffraction patterns for **FJU-101**.

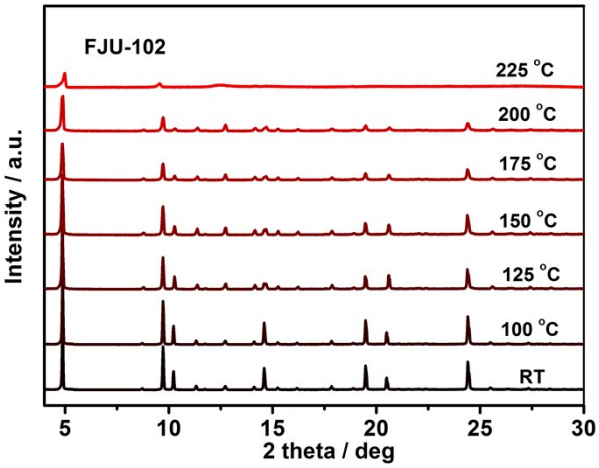

Fig. S7 Variable-temperature powder X-ray diffraction patterns for **FJU-102**.

The variable-temperature PXRD experiment indicates that the host framework structure of **FJU-101** and **FJU-102** both can be retained at temperatures up to 200 °C.

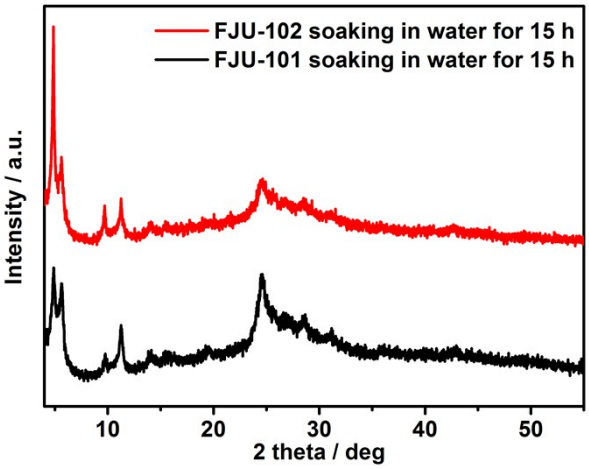

Fig. S8 PXRD patterns of **FJU-101** and **FJU-102** soaked in water for 15 h. They are unstable in water.

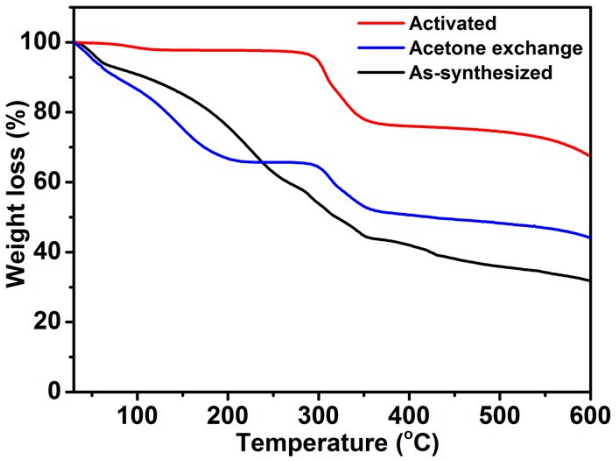

Fig. S9 The TGA curves for **FJU-101** under a nitrogen atmosphere with a heating rate of 10 K min^{-1}.

Thermogravimetric analysis (TGA) for the as-synthesized sample **FJU-101** shows a continuous weight loss of 45.1% from 30 to 295 °C, corresponding to the loss of five DMF, one dioxane and three H_2O molecules in the lattice, and two coordinated H_2O molecules (calcd 44.6%).

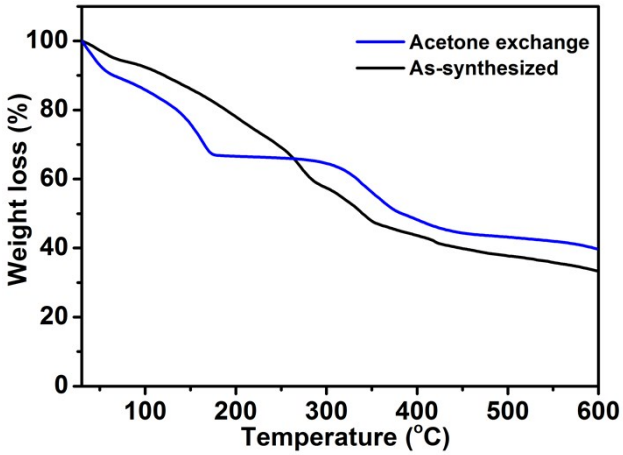

Fig. S10 The TGA curves for **FJU-102**.

Thermogravimetric analysis (TGA) for the as-synthesized sample **FJU-102** shows a continuous weight loss of 44.3% (from 30 to 310 °C) upon heating because of the strong interaction among the high boiling point solvents and the frameworks (calcd 44.2%).

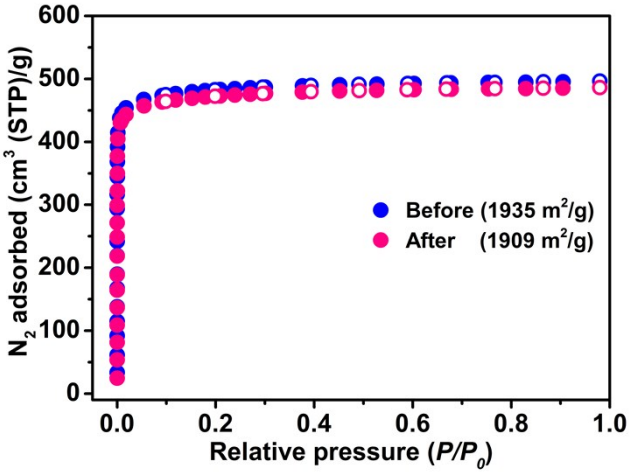

Fig. S11 N_2 isotherms and BET surface areas of **FJU-101a** before and after ethylene uptakes.

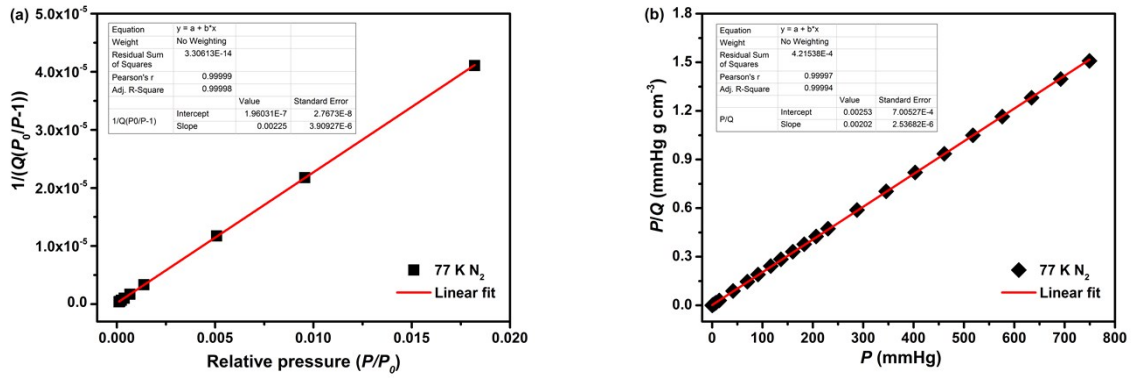

Fig. S12 BET (a) and Langmuir (b) plots for **FJU-101a**.

S_{BET} = 1/(1.96031×10^{-7}+0.00225)/22414×6.023×10^{23}×0.162×10^{-18} = 1935 m^2 g^{-1}

$S_{Langmuir}$ = (1/0.00202)/22414×6.023×10^{23}×0.162×10^{-18} = 2155 m^2 g^{-1}

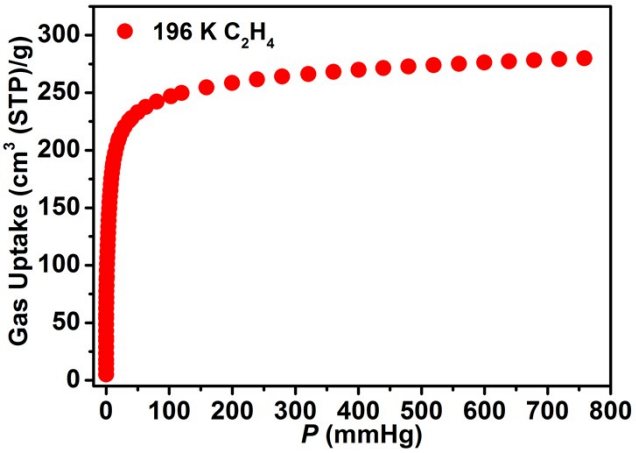

Fig. S13 C_2H_4 adsorption isotherms of **FJU-101a** at 196 K.

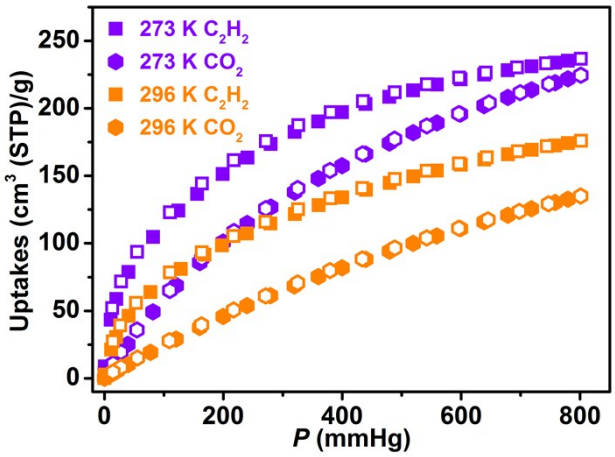

Fig. S14 FJU-101a gas adsorption isotherms for C_2H_2 and CO_2 at 273 K and 296 K under 1 bar.

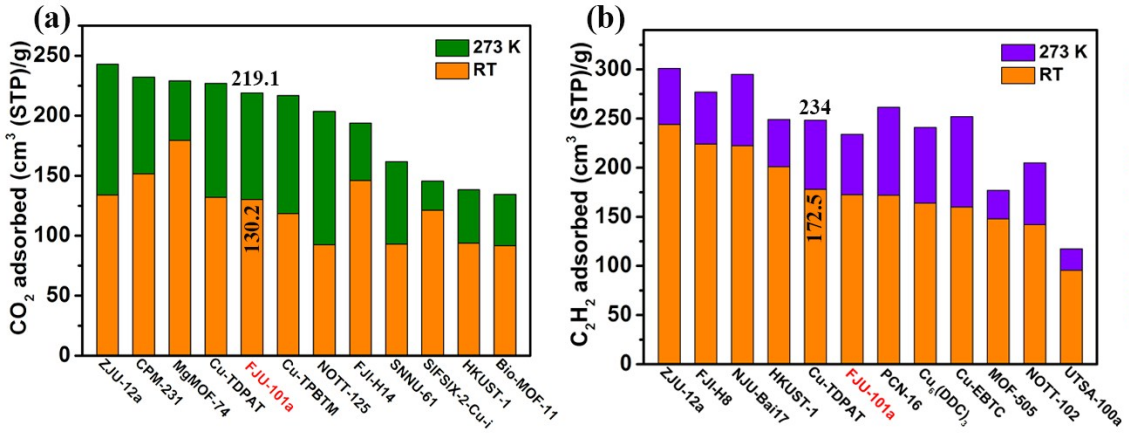

Fig. S15 Comparison of the (a) CO_2 and (b) C_2H_2 uptake capacity of **FJU-101a** with top performing MOFs.

The isosteric enthalpy of adsorption (Q_{st})

The isosteric enthalpy of adsorption for C_2H_2, C_2H_4, and CO_2 was calculated using the data collected at 273 and 296 K. The data were fitted first using a virial-type expression composed of parameters a_i and b_i (eq 1). Then, the Q_{st} (kJ mol^{-1}) was calculated from the fitting parameters using eq 2, where p is the pressure (mmHg), T is the temperature (K), R is the universal gas constant (8.314 J·mol^{-1}·K^{-1}), N is the amount adsorbed (mg g^{-1}), and m and n determine the number of terms required to adequately describe the isotherm.

$$\ln p = \ln N + \frac{1}{T}\sum_{i=0}^{m} a_i N_i + \sum_{i=0}^{n} b_i N_i \qquad (1)$$

$$Q_{st} = -R\sum_{i=0}^{m} a_i N_i \qquad (2)$$

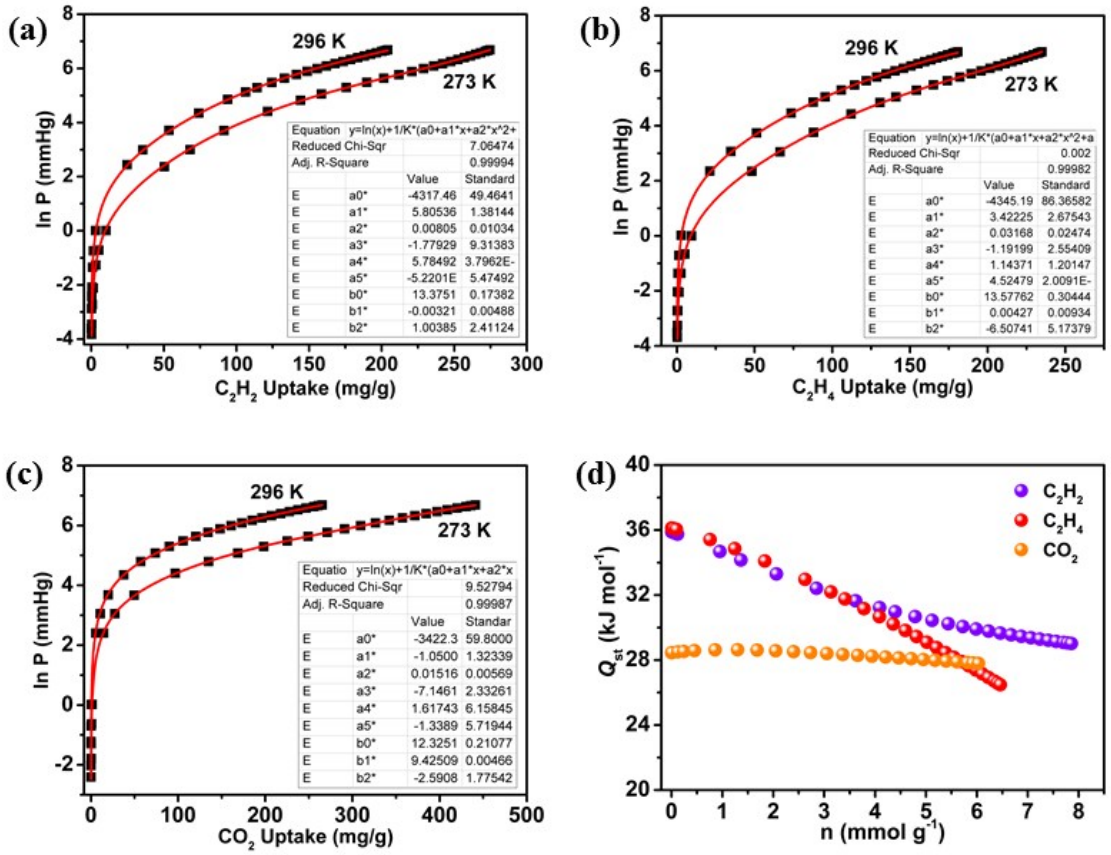

Fig. S16 Experimental data (symbol) and corresponding fittings (solid line) of (a) C_2H_2, (b) C_2H_4 and (c) CO_2 adsorption isotherms of **FJU-101a** at 273 and 296 K. Fit curves are obtained by the virial-type expression.

Prediction of the Gas Adsorption Selectivity by IAST

The ideal adsorption solution theory (IAST) was used to predict the binary mixture adsorption from the experimental pure gas isotherms.[53] To perform the integrations required by IAST, single-component isotherms should be fitted by the correct model. In practice, several methods are available; for this set of data we found that the single-site Langmuir-Freundlich equation was successful in fitting the results.

$$N = N^{\max} \times \frac{bp^{1/n}}{1 + bp^{1/n}} \qquad (3)$$

where p is the pressure of the bulk gas in equilibrium with the adsorbed phase (kPa), N is the amount adsorbed per mass of adsorbent (mmol g^{-1}), N^{max} is the saturation capacities of site 1 (mmol g^{-1}), b is the affinity coefficients of site 1 (1/kPa) and n represents the deviations from an ideal homogeneous surface. The fitted parameters were then used to predict multi-component adsorption with IAST. The adsorption selectivity based on IAST for mixed C_2H_4/N_2 is defined by the following equation:

$$S_{A/B} = \frac{x_A y_B}{x_B y_A} \qquad (4)$$

where x_i and y_i are the mole fractions of component i (i = A, B) in the adsorbed and bulk phases, respectively.

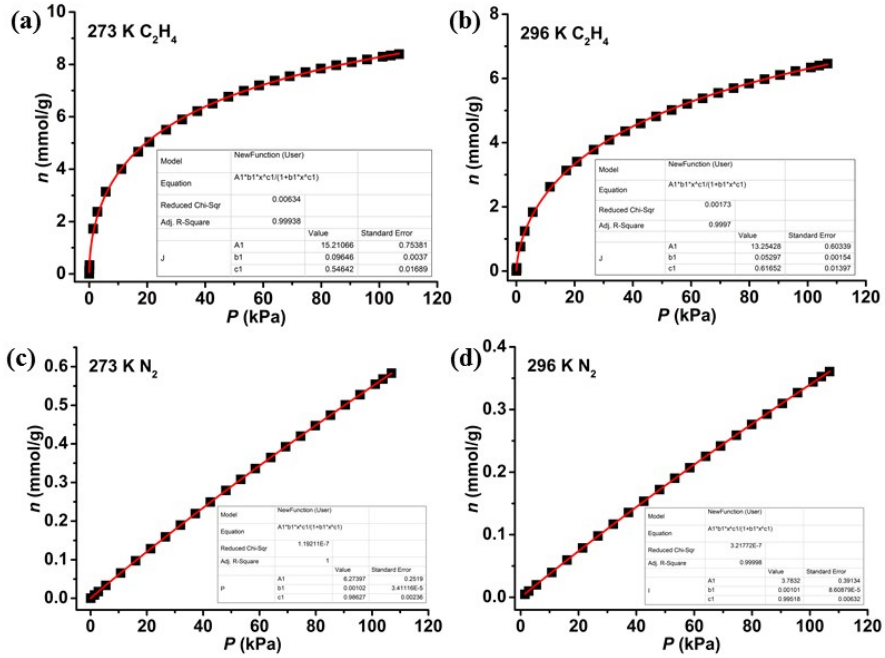

Fig. S17 The graphs of the Single-site Langmuir-Freundlich equations fit for adsorption of C_2H_4 (a, b) and N_2 (c, d) on **FJU-101a** at 273 and 296 K.

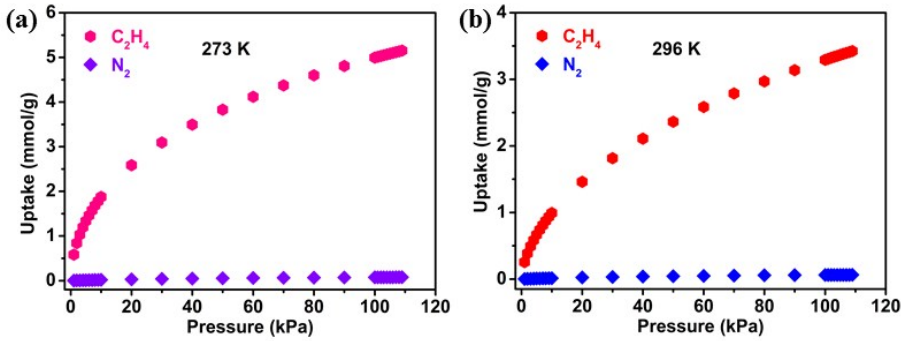

Fig. S18 IAST calculations of mixture adsorption isotherms of **FJU-101a** for 20/80 C_2H_4/N_2 gas mixtures at (a) 273K and (b) 296 K.

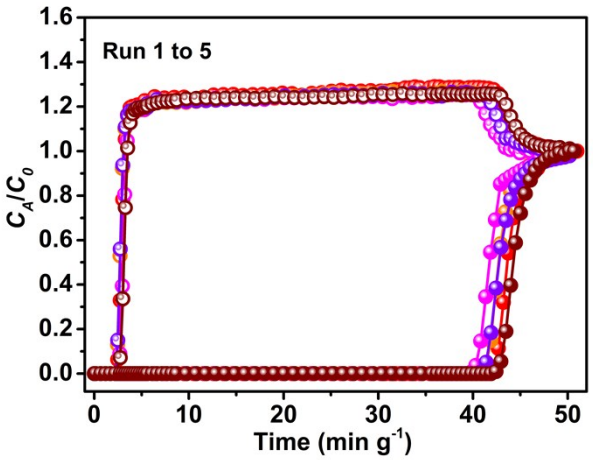

Fig. S19 Cycling column breakthrough curves for C_2H_4/N_2 separation (20/80, v/v) with **FJU-101a** at 296 K and 1 atm. The breakthrough experiments were carried out in a column packed with **FJU-101a** at a flow rate of 6 mL/min.

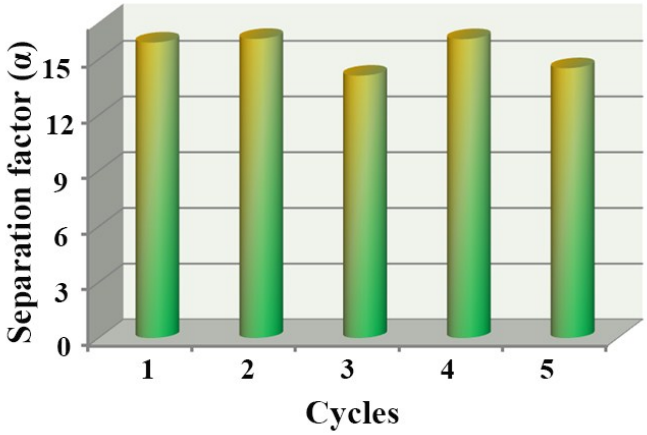

Fig. S20 The recyclability of **FJU-101a** in multiple C_2H_4/N_2 gas mixture breakthrough experiments.

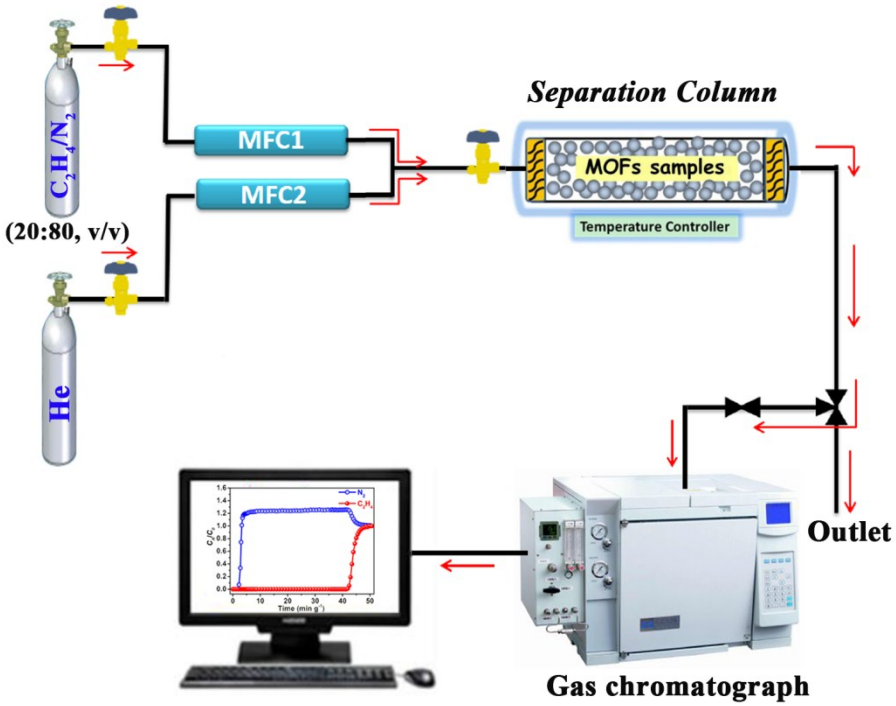

Scheme S1 Illustration of the apparatus for the breakthrough experiments.

Supplementary References

1 X. Duan, Y. Cui, Y. Yang and G. Qian, *CrystEngComm*, 2017, **19**, 1461-1469.

2 Q.-G. Zhai, X. Bu, C. Mao, X. Zhao, L. Daemen, A. J. RamirezCuesta and P. Feng, *Nat. Commun.*, 2016, **7**, 13645.

3 (a) S. R. Caskey, A. G. Wong-Foy and A. J. Matzger, *J. Am. Chem. Soc.*, 2008, **130**, 10870-10871; (b) D. A. Yang, H. Y. Cho, J. Kim, S. T. Yang and W. S. Ahn, *Energy Environ. Sci.*, 2012, **5**, 6465-6473.

4 B. Li, Z. Zhang, Y. Li, K. Yao, Y. Zhu, Z. Deng, F. Yang, X. Zhou, G. Li, H. Wu, N. Nijem, Y. J. Chabal, Z. Lai, Y. Han, Z. Shi, S. Feng and J. Li, *Angew. Chem., Int. Ed.*, 2012, **51**, 1412-1415.

5 B. Zheng, J. Bai, J. Duan, L. Wojtas and M. J. Zaworotko, *J. Am. Chem. Soc.*, 2011, **133**, 748-751.

6 B. Liu, S. Yao, C. Shi, G. Li, Q. Huo and Y. Liu, *Chem. Commun.*, 2016, **52**, 3223-3226.

7 S. Jeong, D. Kim, S. Shin, M. D. Moon, S. J. Cho and M. S. Lah, *Chem. Mater.*, 2014, **26**, 1711-1719.

8 Z. Lu, J. Bai, C. Hang, F. Meng, W. Liu, Y. Pan and X. You, *Chem. - Eur. J.*, 2016, **22**, 6277-6285.

9 D. Lässig, J. Lincke, J. Moellmer, C. Reichenbach, A. Moeller, R. Gläser, G. Kalies, K. A. Cychosz, M. Thommes, R. Staudt and H. Krautscheid, *Angew. Chem., Int. Ed.*, 2011, **50**, 10344-10348.

10 N. H. Alsmail, M. Suyetin, Y. Yan, R. Cabot, C. P. Krap, J. Lü, T. L. Easun, E. Bichoutskaia, W. Lewis, A. J. Blake and M. Schröder, *Chem.- Eur. J.*, 2014, **20**, 7317-7324.

11 I. Spanopoulos, I. Bratsos, C. Tampaxis, D. Vourloumis, E. Klontzas, G. E. Froudakis, G. Charalambopoulou, T. A. Steriotis and P. N. Trikalitis, *Chem. Commun.*, 2016, **52**, 10559-10562.

12 D. De, T. K. Pal, S. Neogi, S. Senthikumar, D. Das, S. S. Gupta and P. K. Bharadwaj, *Chem. - Eur. J.*, 2016, **22**, 3387-3396.

13 Y.-G. Lee, H. R. Moon, Y. E. Cheon and M. P. Suh, *Angew. Chem., Int. Ed.*, 2008, **47**, 7741-7745.

14 L. Liang, C. Liu, F. Jiang, Q. Chen, L. Zhang, H. Xue, H.-L. Jiang, J. Qian, D. Yuan and M. Hong, *Nat. Commun.*, 2017, **8**, 1233.

15 J.-W. Zhang, M.-C. Hu, S.-N. Li, Y.-C. Jiang and Q.-G. Zhai, *Chem. - Eur. J.*, 2017, **23**, 6693-6700.

16 J.-R. Li, J. Yu, W. Lu, L. B. Sun, J. Sculley, P. B. Balbuena and H.-C. Zhou, *Nat. Commun.*, 2013, **4**, 1538.

17 P.-Q. Liao, H. Chen, D.-D. Zhou, S.-Y. Liu, C.-T. He, Z. Rui, H. Ji, J.-P. Zhang and X.-M. Chen, *Energy Environ. Sci.*, 2015, **8**, 1011-1016.

18 P. Nugent, Y. Belmabkhout, S. D. Burd, A. J. Cairns, R. Luebke, K. Forrest, T. Pham, S. Ma, B. Space, L. Wojtas, M. Eddaoudi and M. J. Zaworotko, *Nature*, 2013, **495**, 80-84.

19 T. M. McDonald, W. R. Lee, J. A. Mason, B. M. Wiers, C. Seop Hong and J. R. Long, *J. Am. Chem. Soc.*, 2012, **134**, 7056-7065.

20 (a) X. D. Guo, G. S. Zhu, Z. Y. Li, F. X. Sun, Z. H. Yang and S. L. Qiu, *Chem. Commun.*, 2006, **0**, 3172-3174; (b) Q. M. Wang, D. Shen, M. Bulow, M. L. Lau, S. Deng, F. R. Fitch, N. O. Lemcoff and J. Semanscin, *Microporous Mesoporous Mater.*, 2002, **55**, 217-230; (c) C. R. Wade and M. Dinca, *Dalton Trans.*, 2012, **41**, 7931-7938.

21 J. An, S. J. Geib and N. L. Rosi, *J. Am. Chem. Soc.*, 2010, **132**, 38-39.

22 S. Xiang, Y. He, Z. Zhang, H. Wu, W. Zhou, R. Krishna and B. Chen, *Nat. Commun.*, 2012, **3**, 954.

23 F. Wang, S. Kusaka, Y. Hijikata, N. Hosono and S. Kitagawa, *ACS Appl. Mater. Interfaces*, 2017, **9**, 33455-33460.

24 Y. He, R. Krishna and B. Chen, *Energy Environ. Sci.*, 2012, **5**, 9107-9120.

25 K. Liu, D. X. Ma, B. Y. Li, Y. Li, K. X. Yao, Z. J. Zhang, Y. Han and Z. Shi, *J. Mater. Chem. A*, 2014, **2**, 15823-15828.

26 X. Duan, H. Wang, Z. Ji, Y. Cui, Y. Yang and G. Qian, *Mater. Lett.*, 2017, **196**, 112-114.

27 X. Duan, Y. He, Y. Cui, Y. Yang, R. Krishna, B. Chen and G. Qian, *RSC Adv.*, 2014, **4**, 23058-23063.

28 K. Liu, B. Y. Li, Y. Li, X. Li, F. Yang, G. Zeng, Y. Peng, Z. J. Zhang, G. H. Li, Z. Shi, S. H. Feng and D. T. Song, *Chem. Commun.*, 2014, **50**, 5031-5033.

29 E. D. Bloch, W. L. Queen, R. Krishna, J. M. Zadrozny, C. M. Brown and J. R. Long, *Science*, 2012, **335**, 1606-1611.
30 Y. Liao, L. Zhang, M. H. Weston, W. Morris, J. T. Hupp and O. K. Farha, *Chem. Commun.*, 2017, **53**, 9376-9379.
31 J. Pang, F. Jiang, M. Wu, C. Liu, K. Su, W. Lu, D. Yuan and M. Hong, *Nat. Commun.*, 2015, **6**, 7575.
32 M. Zhang, B. Li, Y. Li, Q. Wang, W. Zhang, B. Chen, S. Li, Y. Pan, X. You and J. Bai, *Chem. Commun.*, 2016, **52**, 7241-7244.
33 H. Wen, H. Wang, B. Li, Y. Cui, H. Wang, G. Qian and B. Chen, *Inorg. Chem.*, 2016, **55**, 7214-7218.
34 C. Song, J. Jiao, Q. Lin, H. Liu and Y. He, *Dalton Trans.*, 2016, **45**, 4563-4569.
35 J. Jiao, L. Dou, H. Liu, F. Chen, D. Bai, Y. Feng, S. Xiong, D.-L. Chen and Y. He, *Dalton Trans.*, 2016, **45**, 13373-13382.
36 T. Xia, J. Cai, H. Wang, X. Duan, Y. Cui, Y. Yang and G. Qian, *Microporous Mesoporous Mater.*, 2015, **215**, 109-115.
37 S. Xiang, W. Zhou, J. M. Gallegos, Y. Liu and B. Chen, *J. Am. Chem. Soc.*, 2009, **131**, 12415-12419.
38 J. Cai, H. Wang, H. Wang, X. Duan, Z. Wang, Y. Cui, Y. Yang, B. Chen and G. Qian, *RSC Adv.*, 2015, **5**, 77417-77422.
39 S. Xiang, W. Zhou, Z. Zhang, M. A. Green, Y. Liu and B. Chen, *Angew. Chem., Int. Ed.*, 2010, **49**, 4615-4618.
40 F. Chen, D. Bai, X. Wang and Y. He, *Inorg. Chem. Front.*, 2017, **4**, 960-967.
41 X. Rao, J. Cai, J. Yu, Y. He, C. Wu, W. Zhou, T. Yildirim, B. Chen and G. Qian, *Chem. Commun.*, 2013, **49**, 6719-6721.
42 X. Cui, K. Chen, H. Xing, Q. Yang, R. Krishna, Z. Bao, H. Wu, W. Zhou, X. Dong, Y. Han, B. Li, Q. Ren, M. J. Zaworotko and B. Chen, *Science*, 2016, **353**, 141-144.
43 J. Cai, Y. Lin, J. Yu, C. Wu, L. Chen, Y. Cui, Y. Yang, B. Chen and G. Qian, *RSC Adv.*, 2014, **4**, 49457-49461.
44 X. Duan, R. Song, J. Yu, H. Wang, Y. Cui, Y. Yang, B. Chen and G. Qian, *RSC Adv.*, 2014, **4**, 36419-36424.
45 Q.-G. Zhai, X. Bu, C. Mao, X. Zhao and P. Feng, *J. Am. Chem. Soc.*, 2016, **138**, 2524-2527.
46 Y. X. Hu, S. C. Xiang, W. W. Zhang, Z. X. Zhang, L. Wang, J. F. Bai and B. L. Chen, *Chem. Commun.*, 2009, 7551-7553.
47 S. H. Yang, A. J. Ramirez-Cuesta, R. Newby, V. Garcia-Sakai, P. Manuel, S. K. Callear, S. I. Campbell, C. C. Tang and M. Schroder, *Nat. Chem.*, 2015, **7**, 121-129.
48 T.-L. Hu, H. Wang, B. Li, R. Krishna, H. Wu, W. Zhou, Y. Zhao, Y. Han, X. Wang, W. Zhu, Z. Yao, S. Xiang and B. Chen, *Nat. Commun.*, 2015, **6**, 7328.
49 J. A. Perman, M. Chen, A. A. Mikhail, Z. Niu and S. Ma, *CrystEngComm*, 2017, **19**, 4171-4174.
50 A. L. Spek, *J. Appl. Crystallogr.*, 2003, **36**, 7-13.
51 L. Sarkisov and A. Harrison, *Mol. Simul.*, 2011, **37**, 1248-1257.
52 (a) J. M. Chin, E. Y. Chen, A. G. Menon, H. Y. Tan, A. T. S. Hor, M. K. Schreyer and J. Xu, *CrystEngComm*, 2013, **15**, 654-657; (b) S. M. Yoon, J. H. Park and B. A. Grzybowski, *Angew. Chem., Int. Ed.*, 2017, **56**, 127-132.
53 A. L. Myers and J. M. Prausnitz, *AIChE J.*, 1965, **11**, 121-127.